

The Memory Effect in Electron Glasses

Eran Lebanon and Markus Müller

*Center for Materials Theory, Serin Physics Laboratory, Rutgers University,
136 Frelinghuysen Road, Piscataway, New Jersey 08854-8019, USA*

We present a theory for the memory effect in electron glasses. In fast gate voltage sweeps it is manifested as a dip in the conductivity around the equilibration gate voltage. We show that this feature, also known as anomalous field effect, arises from the long-time persistence of correlations in the electronic configuration. We argue that the gate voltage at which the memory dip saturates is related to an instability caused by the injection of a critical number of excess carriers. This saturation threshold naturally increases with temperature. On the other hand, we argue that the gate voltage beyond which memory is erased, is temperature independent. Using standard percolation arguments, we calculate the anomalous field effect as a function of gate voltage, temperature, carrier density and disorder. Our results are consistent with experiments, and in particular, they reproduce the observed scaling of the width of the memory dip with various parameters.

PACS numbers: 73.61.Jc

I. INTRODUCTION

In the insulating low temperature phase of dirty semiconductors or granular metallic films the unscreened Coulomb interactions between localized electrons lead to glassy behavior such as slow relaxation, history dependence of observables, non-ergodicity, and memory effects. Even though such “Coulomb glasses” were theoretically predicted more than twenty years ago^{1,2,3,4}, it was a major task to provide convincing experimental evidence for their existence. To our knowledge, very slow electronic relaxation was first reported in the context of capacitance measurements in doped GaAs by Monroe et al.⁵. At temperatures well below 1K, they observed relaxation times that reached the scale of seconds. Even more striking non-equilibrium behavior was found by Ovadyahu’s group in the conductivity of strongly disordered indium-oxide films⁶, where the logarithmic relaxation can extend up to several hours (a typical experimental set-up is shown in Fig. 1). Over the last decade, careful studies of these systems have demonstrated that the electronic out-of-equilibrium behavior is indeed due to the strong frustration induced by the Coulomb interactions between localized electrons, and does not primarily reflect the glassy dynamics of extrinsic degrees of freedom⁷. All the key features usually associated with a glassy system have been observed in these systems: Aging^{8,9}, the dependence of sample properties on its history^{10,11} and memory effects¹². The latter appear as a dip in the film conductivity as the gate voltage is swept through the point at which the system was equilibrated for a long time. The memory of these equilibration conditions usually persists for several hours after the gate voltage has been changed to a new value.

A very similar anomalous field effect, accompanied by slow relaxation, was observed in various granular metals such as Au¹³, Al^{14,15}, as well as Bi and Pb^{16,17}. Furthermore, the aging behavior and the temperature dependence of the memory dip reported in granular Al¹⁸ are very similar to those found in indium-oxide films¹⁹.

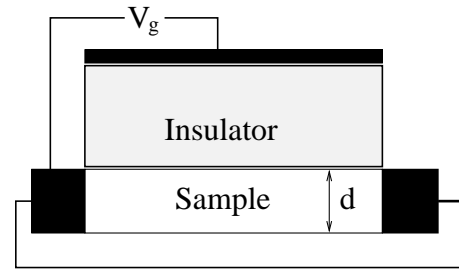


FIG. 1: Typical experimental setup: The sample is a film (semiconductor or granular metal) of thickness d , which is coupled capacitively to a gate electrode. Variation of the gate voltage V_g slightly changes the number of carriers in the film. The conductivity of the sample is probed through contact electrodes that are directly attached to the sample.

This suggests that these glassy effects are rather universal, even though the details of the hopping mechanism and the temperature dependence of the resistivity are clearly different in the two systems.

The anomalous resistance fluctuations observed in ultrathin granular aluminium films¹⁴ and silicon MOSFETs close to the metal insulator transition^{20,21} were also interpreted as indications for glassy behavior. Unfortunately, in these systems, it is difficult to disentangle effects due to intrinsically glassy behavior of interacting electrons from the strong response of the percolating network of hopping electrons to extrinsic slow degrees of freedom.

It has been conjectured that the glassy memory dip reflects a Coulomb gap^{22,23} in the density of states which arises from the unscreened Coulomb interactions. This conjecture is rather natural in the light of recent theoretical work which suggests that the emergence and the universality of the Coulomb gap are related to a glass transition at a finite T_g in these systems^{25,26,27}. This opens the appealing perspective of obtaining more detailed information on Coulomb correlations from a quantitative analysis of the memory experiments.

So far, the precise connection between the memory effect and Coulomb correlations in the electron configuration has remained unclear. The aim of this paper is to provide a quantitative analysis of this effect, assuming a number of glassy properties of the electron system. We start with a review of the glassy features observed in experiments (Section II), concentrating on the memory effect. In Section III, we briefly summarize the theoretical background on the Coulomb gap, hopping transport, percolation theory and glassy behavior which is needed for the quantitative theory of the memory effect in Section IV. The approximations underlying our theory and some open issues are discussed in Section V. We conclude with a brief summary of the main results. Several detailed discussions have been deferred to appendices in order not to interrupt the main line of the reasoning.

II. GLASSY BEHAVIOR IN EXPERIMENTS

A. Slow relaxation and aging

In this section, we discuss some of the experiments exhibiting glassy behavior. Monroe et al.⁵ were the first to observe slow electronic relaxation in the capacitance of p-type doped, partially compensated GaAs. More recently, very slow logarithmic relaxation was observed in the conductivity of various granular metals^{15,16,17}, as well as in indium-oxide films⁷. Furthermore, after equilibration under fixed experimental conditions and subsequent moderate excitation during a time t_w (e.g., by gate voltage⁷ or electric field⁹), the typical relaxation time of such films is found to scale with t_w . This phenomenon, known as simple aging, is observed in many glassy systems such as polymers and supercooled liquids²⁹, as well as spin glasses³⁰.

B. The memory effect

One of the most striking manifestations of the electron glass is the anomalous field effect: After the equilibration of the sample at some gate voltage V_g^0 , subsequent traces of conductivity as a function of gate voltage keep a long-lasting memory of these equilibrium conditions in the form of a symmetric dip around V_g^0 . This dip is superposed on the linear normal field effect due to the increase of carriers, which is usually subtracted and will not be considered further here. In Fig. 2, we illustrate the memory effect - and for the reader more familiar with spin glasses, it is juxtaposed with an analogous experiment that could be done in spin systems.

The fact that the conductivity increases no matter whether carriers are added or depleted, can be understood on a qualitative level by the observation that any perturbation taking the system out of equilibrium must lead to an increase of the conductivity⁶. On a more quantitative level we will have to explain the following exper-

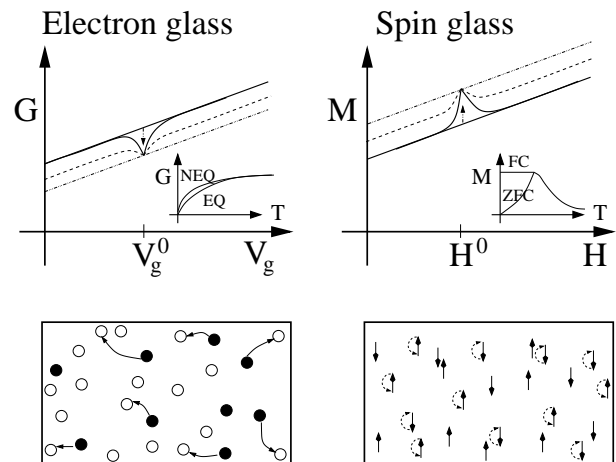


FIG. 2: Left: In an electron glass, the conductivity exhibits a symmetric dip (on top of the linear normal field effect) around the equilibration gate voltage V_g^0 . Far from V_g^0 the conductivity is higher since a fast change of gate voltage takes the system into a higher-lying metastable state. Below a characteristic temperature T_g , there is a clear difference between the conductivity in an “equilibrated” state (EQ) and metastable states (NEQ), see the inset. The relaxation from a metastable state to an “equilibrated” state requires collective electron hops (lower left panel) or crossing of high thermal barriers. Both are so slow that they cannot entirely take place on experimental time scales. However, partial relaxation results in the decrease of the dip amplitude with the sweep rate.

Right: An analogous experiment in spin glasses measures the magnetization as a function of magnetic field H after a slow quench in the equilibration field H^0 . These traces exhibit a peak around H^0 , reflecting that the field cooled magnetization is larger than the magnetization that one obtains after a quench in $H \neq H^0$ and a subsequent switch to H^0 . The inset illustrates this point with the well-known difference between field cooled (FC) and zero-field cooled (ZFC) magnetization as a function of temperature. The relaxation from the ZFC state to the FC state requires the collective rearrangement of many spins (lower right panel).

imental observations extracted from extensive studies on indium-oxide films¹⁰:

(i) The width Γ of the memory dip (measured as a function of density of induced carriers) is remarkably universal. In particular, it is independent of the sweep rate or the application of a magnetic field. Even more surprisingly, it remains unchanged under thermal annealing, a process which reduces the disorder significantly and thus increases the conductivity by several orders of magnitude.

(ii) Γ increases with carrier density.

(iii) Γ increases roughly linearly with temperature, and keeps a certain memory of temperature: After a sudden quench from the equilibration temperature T to a lower temperature $T' < T$, the width Γ relaxes only slowly to the value corresponding to T' , keeping a memory of the larger width characteristic of T ¹².

Note that (ii) is a strong indication for the relevance of electron-electron interactions⁷. Similar results, in particular the decrease of Γ with temperature and memory

of higher temperatures, were recently found in granular aluminium films, too^{15,18}.

We will show in Section IV that these key features can be understood semi-quantitatively with relatively simple arguments on the glassy free energy landscape and the stability of its local valleys.

III. THEORETICAL INGREDIENTS

A. Model

In Anderson insulators, the unscreened Coulomb interactions between the localized carriers are the crucial ingredient which lead to strong electron-electron correlations, the formation of the Coulomb gap and glassy behavior. An approximate description of such systems is given by the classical lattice Hamiltonian^{23,24}

$$H = \sum_i n_i \epsilon_i + \frac{1}{2} \sum_{i,j} \frac{e^2 n_i n_j}{\kappa r_{ij}}, \quad (1)$$

where $n_i = 0, 1$ are the occupation numbers of randomly positioned lattice sites i , and we fix the average occupation to $1/2$. κ denotes the host dielectric constant. The disorder energies ϵ_i are considered as independently and identically distributed random variables with a characteristic width W . This corresponds to a “bare” density of states $\nu_0 \sim 1/r_c^3 W$ where $r_c = n_c^{-1/3}$ is the mean interparticle spacing in a system with carrier density n_c .

Two standard models for semiconductors with localized electrons are usually considered in the literature^{31,32}: the “classical impurity band” (CIB) and amorphous semiconductors (AS). They predominantly differ in the bare density of states ν_0 , see App. A: In the CIB the disorder W is due to randomly distributed charged impurities, so that the disorder is of the order of the nearest neighbor interactions between carriers, and $\gamma \equiv W/(e^2/\kappa r_c) \sim 1$. In the AS, the disorder is due to strong local inhomogeneities, and can be much larger than the nearest neighbor interaction, $\gamma \gg 1$. In indium-oxides, one can tune from the CIB-regime (low n_c) to the AS-regime (high n_c) by controlling the carrier density n_c , the crossover occurring around $n_X \approx \left(\frac{e^2/\kappa}{\hbar^2/2m}\right)^3$.

Most interesting glassy effects have been observed in systems with a high density of carriers: in various granular metals and, most importantly, in indium-oxide. The latter is a highly disordered semiconductor, that can be prepared to have exceptionally high carrier densities in a large range $n_c \approx 10^{19} - 10^{22} \text{cm}^{-3}$, while still being insulating. It is not obvious that these high density systems can still be described by the lattice model (1), since typically the number of carriers per localization volume is larger than one. However, provided the parameter $z \equiv \nu_0 \xi^{D-1} e^2/\kappa$ is small (ξ being the localization length), we can consistently restrict ourselves to a subsystem of well-separated electrons sitting on sites with small ϵ_i ,

which maps the problem onto the effective model (1), as discussed in App. B. We expect that the lattice model remains a reasonable approximation up to $z \approx 1$. Typical values for z in indium-oxides can be estimated to be of the order of $z \approx 0.2 - 0.5$.

B. Coulomb gap and hopping transport

Since the pioneering works by Pollak²², Efros and Shklovskii²³ in the early seventies, it has been known that the unscreened Coulomb interaction in Anderson insulators lead to important correlations in the configuration of electrons, and in particular to the Coulomb gap in the density of states. An upper bound for the single particle density of states in D dimensions is obtained from a self-consistent stability argument^{23,24}

$$\rho(E) \equiv \frac{1}{V} \sum_i \delta(E - E_i) \approx \begin{cases} \alpha_D \left(\frac{\kappa}{e^2}\right)^D E^{D-1}, & E < E_C \\ \nu_0, & E > E_C \end{cases} \quad (2)$$

where

$$E_C = \left((e^2/\kappa)^D \nu_0/\alpha_D\right)^{\frac{1}{D-1}} \quad (3)$$

is the typical scale below which Coulomb correlations dominate over the disorder, and α_D is a numerical constant. In (2), $E_i \equiv dH/dn_i$ is the energy cost to change the occupation on the site i . A very similar distribution of energy costs (but with a substantially larger α_D ^{3,26}) holds for the quasiparticle excitations relevant for variable range hopping, sometimes referred to as electronic polarons^{31,33}. At higher temperature, the Coulomb gap fills in gradually, and is essentially smeared out for $T > E_C$, even though a small depression due to Coulomb correlations should persist.

The presence of a Coulomb gap at low temperatures leads to a crossover of the variable range hopping conductivity form Mott’s law

$$R(T) = R_0 \exp \left\{ \left(\frac{T_M^{(D)}}{T} \right)^{\frac{1}{D+1}} \right\}, \quad (4)$$

with $T_M^{(D)} \sim 1/\nu_0 \xi^D$ to the Efros-Shklovskii law

$$R(T) = R_0 \exp \left\{ \left(\frac{T_{ES}^{(D)}}{T} \right)^{1/2} \right\}, \quad (5)$$

with $T_{ES}^{(D)} \sim e^2/\kappa \xi$. The prefactor R_0 is a slowly varying function of temperature.

One can obtain a quantitative description of variable range hopping from the standard application of percolation theory to a network of Miller-Abrahams resistors formed by pairs of sites^{34,35,36,37}, as reviewed in App. D. In particular, considering an equilibrium quasiparticle

density of states of the form (2) one finds a crossover function

$$\log[R(T)/R_0] = z^{-1/(D-1)}\mathcal{R}(T/T_X), \quad (6)$$

where

$$T_X = (T_{ES}^{D+1}/T_M^2)^{1/(D-1)} \sim z^{1/(D-1)}E_C \quad (7)$$

is the temperature where the conductivity crosses over from Mott's regime to the Efros-Shklovskii regime (see Refs.^{38,39} for similar approaches). In Section IV, we will be concerned with the modification of the conductivity as the density of states is driven out of equilibrium by the application of a gate voltage.

For a long time, experimental evidence for the Coulomb gap in doped semiconductors was only indirect in the form of the Efros-Shklovskii hopping law, and it is difficult to extract detailed information on Coulomb correlations from the temperature dependence of the resistivity $R(T)$ alone. However, *differential* measurements represent direct fingerprints of correlations since they are only sensitive to *changes* in the electron configuration as an external parameter is varied.

In the last ten years, several tunneling experiments on weakly insulating samples provided direct evidence for a pseudogap in the density of states around the Fermi level^{40,41,42,43,44,45,46,47}. However, such experiments are restricted to the regime relatively close to the metal-insulator transition. From this point of view, the analysis of the anomalous field effect represents a convenient method to probe Coulomb correlations also deeper in the insulating regime.

C. Glassiness

A key ingredient to the understanding of the memory effect is the glassiness of the electrons at low temperatures. Such a behavior can be expected from the theoretical consideration that Coulomb systems are very similar to frustrated antiferromagnets, for which recent experiments have demonstrated the existence of a thermodynamic phase transition and spin-glass-like out of equilibrium behavior in almost pure samples⁴⁸.

From numerical simulations, it is well established that at sufficiently low temperatures there is a multitude of metastable states, which are not ergodically connected within timescales accessible in a simulation, since they are separated by large activation or tunneling barriers^{49,50,51,52,53,54}. Extrapolating to experimentally relevant timescales, one expects that a dynamical glass transition takes place in real systems as well.

More theoretical insight can be gained from mean-field theory^{26,27}. Let us first discuss the case of strong disorder ($\gamma > 1$), which corresponds to most experiments in indium-oxide ($n_c \gtrsim n_X$). In 3D systems, a locator approximation to the high temperature expansion predicts

a glass transition at finite temperature²⁶

$$T_g^{(3D)} = \frac{1}{6(2/\pi)^{1/4}}\alpha_3^{1/2}E_C, \quad (8)$$

valid for large disorder, $\gamma \gg 1$. Applying the same approach to 2D systems in the strong disorder limit, one obtains the prediction

$$T_g^{(2D)} = \frac{\sqrt{8\pi}}{\log\left(\frac{\sqrt{\pi/2}}{z}\right)}\alpha_2 E_C^{(2D)}. \quad (9)$$

It is possible that in systems in low dimensions the sharp mean field thermodynamic transition is rounded due to activation over finite but high barriers. In this event, T_g in Eqs. (8,9) is expected to mark the crossover to strongly activated dynamics.

Apart from predicting T_g , mean field theory tells us that in 2D the ratio T_g/E_C (9) can be numerically large, in particular, if we remember that the relevant value of α_2 is the one associated with the quasiparticle density of states. One may therefore expect glassy behavior in strongly disordered films in a substantial range of temperatures $T/E_C > 1$ where the Coulomb gap is hardly developed yet. It is indeed not unusual that the glass transition occurs at a temperature where the density of states does not yet exhibit any of its prominent low temperature features. This is for example the case in the Sherrington-Kirkpatrick model of long range spin glasses where a linear pseudogap starts to open only well below T_g . The same is predicted by the mean field solution for strongly disordered Coulomb glasses.

In the case of moderate disorder, $\gamma \approx 1$ (the CIB model) mean field theory predicts a rather low glass transition temperature²⁷ in 3D,

$$T_g^{(3D)} \approx 0.03 \frac{e^2 n_c^{1/3}}{\kappa}, \quad (10)$$

consistent with the small values found in simulations on irregular lattices without on-site disorder^{55,56}. We expect a similar situation in weakly disordered 2D systems.

In indium-oxide films, a rapid drop of the relaxation time is observed as the carrier density is decreased below $n_{cr} \approx 10^{19} \text{cm}^{-3}$, while keeping the temperature constant⁷. It is possible that this is a manifestation of the glass transition. Indeed, such samples are in the classical impurity band regime ($n_{cr} < n_X$), and Eq. (10) yields a value of T_g close to the measurement temperature of $T_m = 4K$. Films with even lower density, $n_c < n_{cr}$, are still in their ergodic high temperature phase at $T = T_m$, and the relaxation times are unmeasurably fast.

IV. THEORY OF THE MEMORY DIP

A. The density of states as a function of T and V_g

Our theoretical approach is based on the assumption that the metastable states visited after an excitation

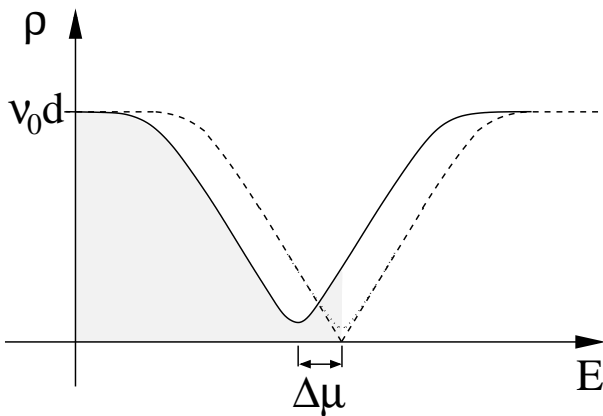


FIG. 3: A sketch of the density of states in a 2D electron glass. The dashed curve corresponds to zero temperature. The dotted curve shows the result of thermal smearing, cf. Eq.(17). The solid curve represents the density of states immediately after applying a gate voltage, cf. Eq.(20). $\Delta\mu$ is the shift of the chemical potential due to the charging of the sample.

by gate voltage reflect the way in which this state was reached. In particular, we argue that at a new gate voltage V_g the (quasiparticle) density of states, and thus the hopping conductivity, will be distinct from the equilibrated state at the same V_g , even if all spontaneous single-particle relaxations had time to take place. The full relaxation to equilibrium will involve multi-particle relaxations and/or processes with high activation energies. Analytical and numerical arguments in support of this scenario have been discussed in Ref.⁵⁷.

Here we are focusing on truly 2D systems, that is, films of thickness $d \lesssim d_{cr} \equiv (\nu_0 e^2 / \kappa)^{-1/2}$ (see App. C for a discussion of the crossover to 3D systems). As discussed in Section III B, the density of states in such films exhibits a linear Coulomb gap at low temperatures. At energies larger than the Coulomb correlation scale $E_C = (e^2 / \kappa)^2 \nu_0^{(2D)} / \alpha_2$, the density of states approaches the constant bare density of states $\nu_0^{(2D)} = \nu_0 d$. We describe this crossover (for $T = 0$) by the interpolating function

$$\rho_0(E) = \nu_0^{(2D)} \tanh|E/E_C|, \quad (11)$$

whose precise form is, however, not essential for the following analysis.

At finite temperature some electrons are excited out of their local equilibrium position, which induces fluctuations in the (single electron) site energies, $E_i = \epsilon_i + \sum_{j \neq i} e^2 n_j / \kappa r_{ij}$:

$$E_i = E_i^{(0)} + \delta\phi_i \quad (12)$$

where

$$E_i^{(0)} = \epsilon_i + \sum_{j \neq i} e^2 n_j^{(0)} / \kappa r_{ij} \quad (13)$$

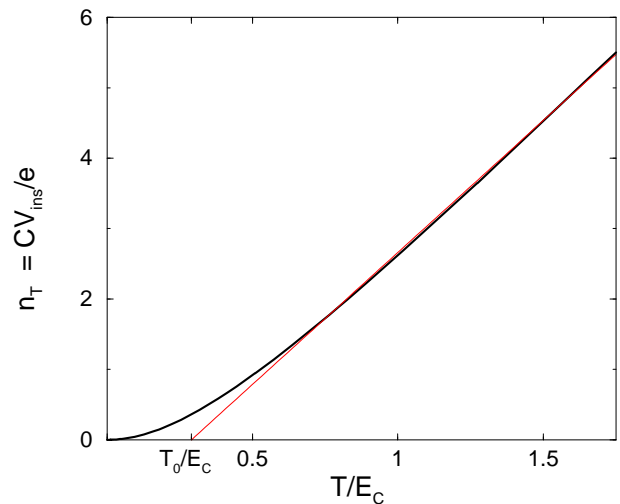


FIG. 4: (Color online) The density of thermally excited carriers, n_T , as a function of temperature, or, equivalently, the gate voltage difference CV_{ins}/e at which the anomalous field effect saturates. At high temperature, V_{ins} is linear in T [$\propto (T - T_0)$], and scales as T^2 at low temperatures. n_T and CV_{ins}/e are plotted in units of $zE_C\nu_0 d$.

is the energy cost to change the occupation of site i in the locally stable configuration characterized by $\{n_i^{(0)}\}$, and

$$\delta\phi_i = \sum_{j \neq i} e^2 \delta n_j / \kappa r_{ij} \quad (14)$$

are potential fluctuations due to thermally activated changes in the occupation δn_j . In a first approximation we assume the $\delta\phi_i$'s to be independent Gaussian distributed variables with variance $\langle \delta\phi^2 \rangle = \alpha_T n_T (e^2 / \kappa)^2$,

$$P_T(\delta\phi) = \frac{\kappa}{e^2} \frac{1}{\sqrt{\pi \alpha_T n_T}} \exp \left\{ -\frac{\kappa^2}{e^4} \frac{\delta\phi^2}{\alpha_T n_T} \right\}, \quad (15)$$

where $\alpha_T = O(1)$ is a numerical factor and n_T is the density of thermally excited electrons

$$n_T = \int_{-\infty}^0 dE \rho_0(E) (1 - f(E)) + \int_0^{\infty} dE \rho_0(E) f(E), \quad (16)$$

f being the Fermi distribution. Note that at high temperatures n_T is linear in T , while at low temperatures it approaches zero as $n_T \sim T^2$ (see Fig. 4).

As a consequence of these fluctuations, the density of states is smeared. In the approximation of independent shifts $\delta\phi_i$, it is described by the convolution

$$\rho(E, T) = \int d(\delta\phi) P_T(\delta\phi) \rho_0(E - \delta\phi). \quad (17)$$

Upon application of a gate voltage V_g , new carriers are introduced into the system. It is reasonable to assume them to rapidly occupy the empty sites with the lowest energies E_i available. Sometimes, the occupation of a

site may cause a small number of neighboring particles to hop slightly away, to reduce the energy of the system. Considering the introduction of the new particle and such local rearrangements as one composite process, one may say that the new carriers actually occupy “quasiparticle” states (very similar to the electronic polarons relevant for conductivity³³). However, even though the thus reached state may be stable to single particle relaxations, it will in general be an excited state under the new gate voltage. Only if the system is given a long time to equilibrate, it will relax to the new ground state, which involves multiparticle transitions or the crossing of high activation energies.

In order to describe the quasiparticle density of states analytically, we assume that the latter type of relaxation processes has not had time to occur. Furthermore, we assume that apart from the local response of nearby particles, the introduction of new carriers does not trigger major rearrangements of the electron configuration. This will be justified further below. A more thorough investigation of these assumptions can be found in⁵⁷.

Under these assumptions, the effects of the gate voltage are twofold: (i) the new carriers successively fill the empty (quasiparticle) levels close to the Fermi energy, shifting the chemical potential to $\mu + \Delta\mu$, while the minimum in the density of states remains at the old value of μ (cf. Fig. 3); (ii) the extra particles further smear the density of states, similarly to the thermal effect described above. They induce further energy shifts $\delta\phi_i$, which we take to be randomly distributed according to

$$P_{V_g}(\delta\phi) = \frac{\kappa}{e^2} \frac{1}{\sqrt{\pi\alpha_V C V_g/e}} \exp\left\{-\frac{\kappa^2}{e^4} \frac{(\delta\phi - \Delta\mu)^2}{\alpha_V C V_g/e}\right\}, \quad (18)$$

where $\alpha_V = O(1)$ and C is the capacitance per unit area. We have also accounted for the global shift in chemical potential $\Delta\mu$, which is related to the gate voltage by

$$C V_g = e \int_0^{\Delta\mu(V_g)} dE \rho(E). \quad (19)$$

Notice that in the presence of a Coulomb gap, the dependence of $\Delta\mu$ on V_g is non-linear. The density of states after a sudden gate voltage change is finally obtained as

$$\rho(E, T, V_g) = \int d(\delta\phi) P_{V_g}(\delta\phi) \rho(E - \delta\phi, T, V_g = 0). \quad (20)$$

The density of states at different stages of smearing is shown in Fig 3. Below, we will use the density of states (20) to calculate quantitatively the out of equilibrium conductivity

Note that in assumption (i) it is implied that new carriers will occupy sites across the whole film. This is only justified if the film thickness is of the order of the screening length of the sample. In the absence of a Coulomb gap the latter can be estimated as $l_{sc} \sim (\nu_0 e^2 / \kappa)^{-1/2}$ which is of the same order as the thickness d_{cr} which governs the crossover to a 3D system. (However, in the presence of

an Efros-Shklovskii Coulomb gap, the screening length is probably substantially larger on intermediate timescales, as suggested by the capacitance experiments of Ref.⁵.) We believe that in films thicker than l_{sc} , the anomalous field effect is mostly due to the filling of states within a screening length from the surface. The quantitative theory below does not strictly apply to this case. However, the instability argument given in the following subsection should still hold, provided the film thickness d is replaced by $d_{cr} \sim l_{sc}$.

B. Instability criterion and breakdown of memory

The description (20) of an adiabatic response to the change of gate voltage V_g , without any relaxation of the electron configuration, is applicable only for small enough values of V_g . As the gate voltage is increased, more and more new particles are introduced into the sample and reshuffle the site energies, until at a certain scale ($V_g = V_{ins}$) the local minimum in which the system resides becomes unstable. For higher gate voltages the system will relax to a new local minimum whose density of states is no longer described adequately by the adiabatic smearing and shifting of Eq. (20) alone. As long as the Coulomb gap is not strongly developed, it is reasonable to assume that the new local minimum represents a rather generic metastable state relatively high up in the energy spectrum of all possible states. We then expect that the conductivity will not significantly change upon further increase of the gate voltage, since the system remains in the high energy spectrum of states. However, such a new metastable state will still have a large configurational similarity (or “overlap” in spin glass language) with the original ground state: Most of the sites that were occupied in the original local state remain occupied in the new local minimum. The memory of the original configuration is thus preserved. In particular, when the gate voltage is swept back to its original value, the low equilibrium conductivity will be recovered. As the gate voltage is increased beyond the instability scale V_{ins} , the overlap of the new local minimum with the original state continuously decreases and the memory of the original state is gradually lost. This will be manifested by the disappearance of the memory dip once the gate voltage is swept beyond a scale V_{mem} .

Let us now analyze in more detail what determines the instability scale V_{ins} . It is reasonable to expect that as long as the density of carriers introduced by the gate is smaller than the density of thermally excited electrons n_T , the gate voltage effect is perturbative, which justifies our adiabatic treatment of the density of states. This reasoning implies $C V_{ins} \gtrsim e n_T$.

On the other hand, at gate voltages $C V_g > e n_T$ the shift in chemical potential is of the order of the temperature $\Delta\mu \sim T$, and accordingly, the new carriers are introduced on sites that were essentially empty in the original state. The local environment of those sites will gener-

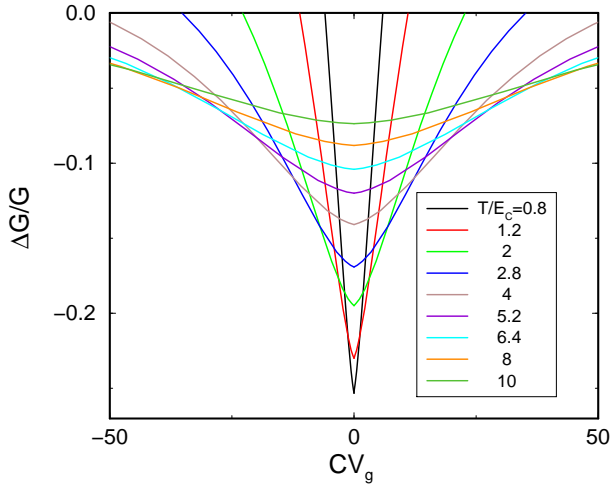


FIG. 5: (Color online) Memory dip as a function of gate voltage for $z = 0.4$ and various temperatures of the order of E_C and higher. We plot the relative change in conductivity with respect to its asymptotic value at large gate voltages, $\Delta G/G = [G(V_g) - G(V_{\text{ins}})]/G(V_{\text{ins}})$. The cusp width is proportional to temperature, and its amplitude decreases as temperature is increased. CV_g is plotted in units of $ezE_C\nu_0d$

ally not be favorable to the addition of a new particle. Rather, the newly introduced electron will trigger fast relaxation processes and destabilize the original state. In other words, the configuration generated by occupying more and more levels will soon become a generic high energy state for $CV_g > en_T$. In summary, we expect an instability and thus a saturation of the out-of-equilibrium conductivity at

$$V_{\text{ins}} \approx \frac{en_T}{C} \approx \frac{e\nu_0d}{C} \times \begin{cases} \pi^2 T^2 / 6E_C, & T \ll E_C \\ 2\ln 2 T - \Omega / 2\nu_0d, & T > E_C \end{cases} \quad (21)$$

where $\Omega = \int dE(\nu_0d - \rho(E)) \sim \nu_0dE_C$ is the total deficit of density of quasiparticle states due to the presence of a Coulomb gap. In Fig. 4 we plot V_{ins} as a function of temperature.

As explained above, we expect the memory dip to saturate around the instability scale, its total width being roughly $\Gamma = 2V_{\text{ins}}$. A linear high temperature behavior $\Gamma \sim T \approx T_0$ was indeed observed experimentally⁵⁸. Equation (21) further predicts the interesting relation $T_0 = \int dE(1 - \rho(E)/\nu_0d)/4 \ln 2$, which allows to determine experimentally the width of the Coulomb gap.

The memory of the equilibrium state is essentially erased once the gate voltage has exceeded a certain scale $V_{\text{mem}} > V_{\text{ins}}$. We expect this crossover to occur when the random energy shifts $\delta\phi_i$ are comparable to the Coulomb correlation scale, $\langle \delta\phi^2 \rangle^{1/2} \approx E_C$. More explicitly, we obtain the estimate

$$V_{\text{mem}} \approx \zeta_V \frac{e\nu_0d}{C} E_C, \quad (22)$$

which is temperature independent contrary to V_{ins} . The numerical factor $\zeta_V = O(1)$ is presumably numerically

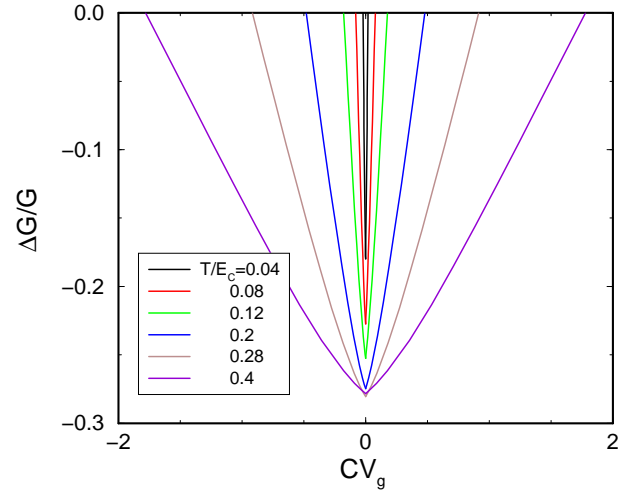


FIG. 6: (Color online) $\Delta G/G = [G(V_g) - G(V_{\text{ins}})]/G(V_{\text{ins}})$ plotted against gate voltage for low temperatures, $T < E_C$, and $z = 0.4$. In this regime, the cusp width increases quadratically with temperature. The adiabatic percolation treatment predicts the amplitude of the cusp to increase with temperature. This is probably an artifact, see the discussion in Section V. CV_g is plotted in units of $ezE_C\nu_0d$.

large (at least of the order of T_g/E_C which may be appreciable in strongly disordered 2D systems, cf. (9)).

In Ref.¹¹ the authors reported that the ratio $V_{\text{mem}}/V_{\text{ins}}$ is not a universal number (at fixed temperature), but increases with carrier density. The above arguments indeed suggest that at high temperatures, $T \gtrsim E_C$,

$$\frac{V_{\text{mem}}}{V_{\text{ins}}} \propto \frac{E_C}{T - T_0}. \quad (23)$$

At fixed temperature, this ratio increases with carrier concentration, as E_C does.

C. Non-equilibrium conductivity

For gate voltages $V \lesssim V_{\text{ins}}$ we can calculate the non-equilibrium conductivity from the modified density of states, Eq. (20), and the percolation criterion of App. D. Assuming that the conductivity saturates to G_∞ beyond the scale V_{ins} , we may estimate $G_\infty \approx G(V_g = V_{\text{ins}})$ from which we obtain the amplitude of the memory dip as $\Delta G \equiv G_\infty - G(0) \approx G(V_{\text{ins}}) - G(0)$.

The smearing of the density of states due to new carriers has a minor effect on the non-equilibrium conductivity since it mostly affects energy scales on the order of the temperature whereas the energy range probed by variable range hopping is much larger. However, the shift of the chemical potential, $\Delta\mu$ is the crucial out-of-equilibrium feature which leads to the increase of the conductivity.

The results we obtained from the percolation treatment confirm the general assertion⁸ that the conductivity always increases with $|V_g|$. In Fig. 5 we plot the relative change of the conductivity $\Delta G(V_g)/G_\infty$ for high

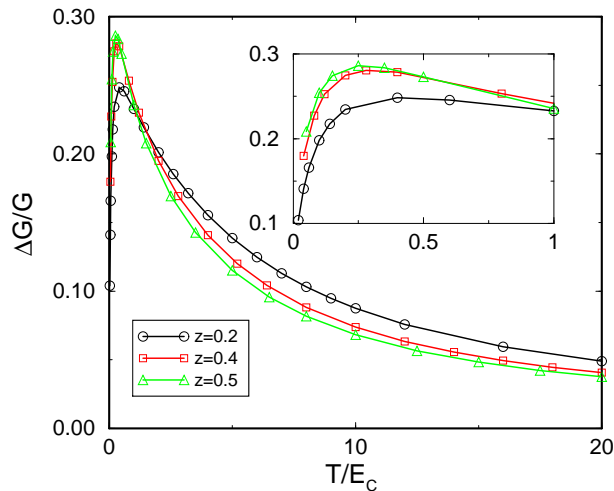


FIG. 7: (Color online) The relative amplitude of the conductivity dip $[G(V_{\text{ins}}) - G(0)]/G(V_{\text{ins}})$ as a function of temperature for various values of z . Inset: Low temperature behavior of the relative amplitude for the same values of z .

temperatures $T_g > T \gtrsim E_C$. This is the temperature regime in which most experiments on indium-oxide films are performed. The cusp width decreases linearly with temperature while its amplitude increases, an asymptotic analysis yielding

$$\frac{\Delta G}{G} \sim \frac{E_C}{T}, \quad (24)$$

see Fig. 7.

At low temperature, $T < E_C$, the cusp width increases quadratically with T . In contrast to the high temperature regime, the adiabatic percolation treatment combined with the instability criterion predict $\Delta G/G_\infty$ to increase with temperature as

$$\frac{\Delta G}{G} \sim \sqrt{\frac{T}{T_{ES}}}. \quad (25)$$

The full functions $\Delta G(V_g)/G_\infty$ are shown in Fig. 6.

The *absolute* amplitude of the dip, ΔG , is found to be a non-monotonic function of temperature, as shown in Fig. 8. The non-monotonicity is more pronounced in less resistive films (see the curves for the localization parameters $z = 0.4, 0.5$) where a clear peak appears in ΔG at T_{max} , while for more resistive films ($z = 0.2$) this feature is hard to discern. Very similar non-monotonic behavior of ΔG was observed experimentally¹⁹.

V. DISCUSSION

A. Low temperature behavior

The non-monotonic behavior of the *relative* amplitude predicted by Eqs. (24,25) was not observed in experiments so far. Even though this might be due to the fact

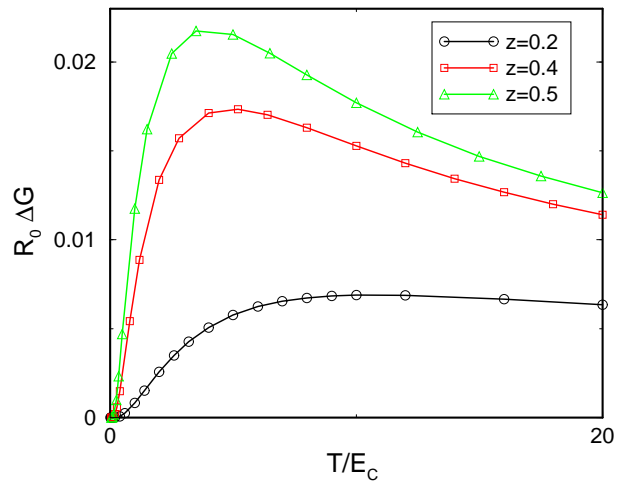


FIG. 8: (Color online) Amplitude of the conductivity dip $G(V_{\text{ins}}) - G(0)$, as a function of temperature for $z = 0.2, 0.4$ and 0.5 . Less resistive films (larger z) exhibit a clear maximum at relatively high temperatures.

that most experiments are performed at high temperatures, we believe the prediction $\Delta G/G \rightarrow 0$ for $T \rightarrow 0$ to be an artifact for the following reasons: (i) One can trace back the origin of the prediction $\Delta G/G \sim T^{1/2}$ to the conservation of the total deficit of density of states under the application of a gate voltage. In our approximation, this is a simple consequence of only shifting and convoluting the density of states. However, it is likely that for $V \sim V_{\text{ins}}$ the neglected fast relaxation processes destroy this exact conservation, which would lead to the saturation of $\Delta G/G$ at low temperatures. (ii) The assumption that the asymptotic conductivity G_∞ is well estimated by the non-equilibrium conductivity at V_{ins} is probably incorrect at very low temperatures. In order to illustrate this point, let us consider a large gate voltage V_L with $V_{\text{ins}} \ll V_L \leq V_{\text{mem}}$, such that the shift of the chemical potential is of the order of E_C . This will take the system into a high energy state where fast relaxation processes lead to the formation of a new Coulomb gap. The sites within the new gap will be mostly different from the sites in the old one, and it is likely that the total deficit of density of states in this new Coulomb gap is initially smaller than the one in the equilibrium state. More precisely, one may expect that the linear slope α_{ES}^{2D} of the density of states in the new configuration is slightly larger than that in the ground state, and the corresponding Efros-Shklovskii temperature T_{ES} is smaller accordingly (see App. D). This would suggest that $\Delta G/G$ scales like $T^{-1/2}$ and thus *increases* with decreasing temperature. In this temperature regime, one may expect an additional increase of conductivity with increasing gate voltage, even beyond the instability point V_{ins} . The description of the conductivity in that regime would require to take into account partial relaxation processes which goes beyond the present approach. However, it remains open whether the \sqrt{T} behavior Eq. (25) ap-

plies in an intermediate range of temperatures.

B. Comparison to experiments

1. The memory dip

As described in Section IV C, the adiabatic percolation approach reproduces well the temperature dependence of several key features of the memory dip. In particular, we showed that one may infer the width of the quasiparticle Coulomb gap from a careful study of the temperature dependence of the width. Moreover, from Eq. (21) we see that the width of the memory dip should be proportional to the bare density of states ν_0 , which increases with carrier concentration as discussed in Section III A: In the impurity band regime, $n_c < n_X$, one expects $\nu_0 \sim n_c^{2/3}$, while for large carrier concentration the density of states crosses over to a free electron-like behavior $\nu_0 \sim n_c^{1/3}$. This scenario agrees rather well with the observed bending of the dip width as a function of carrier density in indium-oxide films⁷.

At high temperatures, the percolation approach predicts a decrease of the cusp amplitude like $1/T$, which is weaker than what is usually observed in experiments^{15,19}. This difference may again originate from our neglect of spatial correlations in $\delta\phi_i$ discussed above. Even more likely is the scenario that our assumption of homogeneously glassy samples breaks down at higher temperatures. Indeed, if only a few rare regions with stronger disorder remain glassy their effect on the out of equilibrium conductivity might be strongly reduced due to shortcuts by non-glassy regions.

Let us briefly discuss the effect of varying the disorder strength or applying a magnetic field. Experimentally, both changes seem not to affect the width of the memory dip. Furthermore, even strong magnetic fields change the amplitude $\Delta G/G$ only slightly. These experimental observations are quite surprising since both the variation of disorder and magnetic field affect the conductivity G itself appreciably.

The first observation can be naturally explained within our picture if we assume that changing the disorder (by annealing) or applying a magnetic field mostly affects the localization length without altering the bare density of states ν_0 . Since the instability criterion originates from a static consideration within the classical model Hamiltonian (1), it is insensitive to the localization length. The width of the memory dip remains thus constant under variations of disorder or magnetic field.

The near constancy of $\Delta G/G$ with magnetic field is more subtle. In terms of the percolation approach the variation of the localization length simply changes the parameter z , while leaving E_C fixed. From Fig. 7, it can be seen that the effect of z on $\Delta G/G$ is indeed relatively small, while the corresponding change of ΔG (cf. Fig. 8) is much more important.

2. Memory of temperature

An interesting effect of temperature memory was reported both for the indium-oxide films¹², and for films of granular aluminum¹⁸. After equilibration at $V_g = 0$ and temperature T_0 , the system is quenched to $T_1 < T_0$, and the conductivity is probed as a function of gate voltage before the sample equilibrates. In this protocol, the anomalous field effect maintains the characteristic width of the initial temperature T_0 for a rather long time before narrowing down.

This effect can be understood in terms of the instability criterion proposed above: The energy minima or valleys in which the electron glass typically settles at temperature T_0 will be stable upon injection of additional carriers up to the critical density n_{T_0} . After a temperature quench the system will in general remain in this valley, and the stability threshold of the higher temperature will be preserved temporarily. Finally, slow relaxation processes allow the system to dig itself deeper down into a subvalley of the energy landscape, since the thermal fluctuations are now smaller. These lower lying states will have a reduced stability threshold, as will be reflected by a smaller dip width Γ .

C. Observability of glassy effects in doped semiconductors

So far, slow electronic relaxation was observed only in very few cases of moderately doped semiconductors⁵. The natural question thus arises as to why glassy effects, such as in indium-oxide, are not more frequently encountered. The reason is most likely that many standard semiconductors have relatively low carrier concentrations with well localized electrons. Such systems are described by the classical impurity band model whose glass transition in 3D is suppressed by a small numerical factor, see Eq. (10). Estimating the Efros-Shklovskii conductivity at that temperature scale, one finds

$$\ln(R/R_0) \approx \left(C_{ES}^{(3D)} \frac{e^2}{\kappa \xi T_g} \right)^{1/2} \approx \left(\frac{C_{ES}^{(3D)} n_c^{-1/3}}{0.03 \xi} \right)^{1/2}, \quad (26)$$

which is very large even when the localization length approaches the inter-impurity distance. This makes the detection of glassy effects in the hopping conductivity nearly impossible, due to the intrinsically large noise in such systems. However, glassiness should still be observable in static quantities, such as the capacitance measurements of Ref.⁵.

In amorphous semiconductors with relatively high carrier concentration glassy effects as described in this paper should generally be observable. The same is true for doped semiconductors sufficiently close to the metal insulator transition.

Once the localized wavefunctions start to overlap significantly ($z > 1$) one may expect the nature of the glass

phase to change and finally disappear completely. Many recent experiments probing the Coulomb gap are actually carried out in this regime^{46,47,59}. They reveal very interesting quantum critical behavior associated with the metal insulator transition, but have not thoroughly investigated the glassy aspects of the samples so far. First attempts towards a theoretical description of glassiness in the regime close to the transition were undertaken in Refs.^{60,61}. At this point it remains an interesting open question, both theoretically and experimentally, whether the onset of metastability and glassiness coincides with the transition to the insulator, and, if so, what role the glassy freezing plays in the physics of the metal-insulator transition.

VI. CONCLUSION

We have analyzed the memory effect in electron glasses. The non-equilibrium conductivity was calculated within a percolation approach, assuming the local metastability of the glass state. This allowed us to describe the anomalous field effect quantitatively, reproducing many of the experimental characteristics observed in indium-oxides and granular aluminum. We have provided a simple physical picture for the voltage scales at which the memory dip saturates and erasure of memory occurs, respectively. We argue that the saturation scale increases with temperature, its dependence on temperature reflecting the characteristics of the Coulomb gap. We have predicted the ratio of the two voltage scales as a function of temperature and carrier density, which can be tested in experiments.

VII. ACKNOWLEDGMENTS

We acknowledge discussions with P. Chandra, M. Feigel'man, M. Gershenson, T. Grenet, L. Ioffe, Z. Ovadyahu and B.I. Shklovskii. We thank L. Ioffe and Z. Ovadyahu for the continuous encouragement and interest in our work, as well as for the frequent exchange of ideas. E.L. was supported by DOE grant DE-FE02-00ER45790. M.M. was supported by NSF grant DMR 0210575.

APPENDIX A: THE BARE DENSITY OF STATES OF SEMICONDUCTORS

In this appendix we derive approximate expressions for the bare density of states in semiconductors and granular metals.

In the literature, two standard models for semiconductors with localized electrons have been considered, see Refs.^{31,32} for a review. The ‘‘classical impurity band’’ model refers to lightly doped, partially compensated semiconductors where all carriers are localized within

a Bohr radius around majority impurities. Due to the Coulomb interactions with randomly distributed charged impurities, the on-site energies ϵ_i of these localized states are scattered over a range of the order of the nearest neighbor interactions, $e^2/\kappa r_c$, where $r_c \equiv n_c^{-1/3}$ is the average distance between carriers, n_c is the carrier density (uncompensated dopant concentration) and κ is the host dielectric constant. Accordingly, the bare density of localized states (which neglects Coulomb interactions between the localized carriers) is of the order of

$$\nu_0 = \frac{n_c}{e^2/\kappa r_c} = \frac{\kappa}{e^2} n_c^{2/3}, \quad (\text{impurity band}). \quad (\text{A1})$$

The second frequently considered model describes amorphous semiconductors in which the disorder of the on-site energies ϵ_i is due to strong local inhomogeneities. In this case, their scatter is usually much larger than that introduced by Coulomb interactions with impurities. As a consequence, the bare density of states is lower than (A1), as schematically illustrated in Fig. 9.

The set of localized states does not need to fill the whole region between the valence and the conduction band. In the case of indium-oxide (both amorphous⁶² and crystalline⁶³), it has been established that the localized states form a tail joining the conduction band at the mobility edge. Furthermore, it was found that at sufficiently high carrier densities, the density of states in the range of localized states is in surprisingly good agreement with free-electron estimates,

$$\nu_0 \approx \frac{n_c}{\hbar^2 n_c^{2/3}/2m}, \quad (\text{high density, } n_c > n_X). \quad (\text{A2})$$

This reflects the fact that the kinetic energy $E_{kin} = \hbar^2 k_F^2/2m \sim \hbar^2 n_c^{2/3}/2m$ of the localized wavefunctions dominates over the effects of inhomogeneities in the electrostatic potential. Note, however, that a crossover to the regime of dominant Coulomb interactions (Eq. (A1)) is to be expected around $n_c \approx n_X$ where $E_{kin} \approx e^2 n_c^{1/3}/\kappa$, i.e.,

$$n_X \approx \left(\frac{e^2/\kappa}{\hbar^2/2m} \right)^3. \quad (\text{A3})$$

In granular metals, the role of the localized sites in the model (1) is taken by the grains. As a consequence of impurities and the disorder in the size and the arrangement of the grains, the cost to introduce one more particle on a grain is a random quantity of the order of the typical charging energy E_C or the level spacing δ in the grain, whichever is larger. Usually the charging energy will dominate, unless the grains are very small or the effective dielectric constant of the metallic film is very large. The random on-site energies ϵ_i entering the Hamiltonian (1) are therefore scattered with a typical width $W = \max[E_C, \delta]$, and the effective bare density of states can be estimated as

$$\nu_0 \approx \frac{n_c}{\max[E_C, \delta]}, \quad (\text{granular metals}) \quad (\text{A4})$$

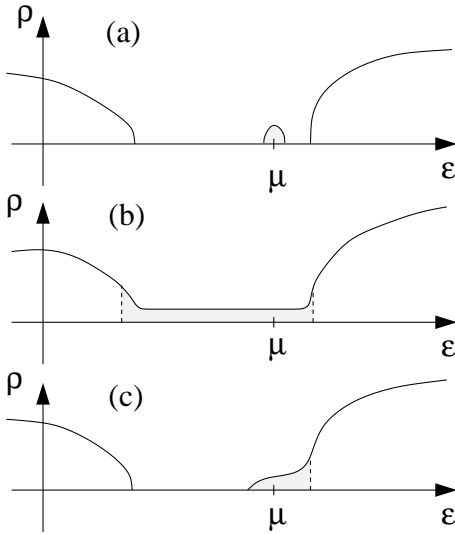


FIG. 9: Schematic view of the bare density of states (neglecting electron-electron interactions) in different classes of semiconductors: a) classical impurity band (lightly doped semiconductors) b) strongly disordered amorphous semiconductor (e.g., amorphous germanium), c) doped, disordered semiconductor with localized band tails at the bottom of the conduction band (e.g., indium-oxide).

which is typically a few times smaller than the (2D) density of states in a bulk metal.

APPENDIX B: REDUCTION OF HIGH DENSITY SYSTEMS TO THE STANDARD MODEL

Here we examine under which condition a high density system can be described by the classical Hamiltonian (1). The aim is to consider only a strip of localized states of width ΔE around the chemical potential, and to work with an effective model of occupied and empty levels within this strip. In this approximation, the carriers localized in states of lower energy are considered inert in the sense that they do not hop to other sites. Notice however, that such “core” electrons may still have fairly extended wavefunctions, and therefore contribute to the polarizability of the medium, renormalizing the host dielectric constant.

The mapping of such an energy strip to a model of point-like localized states (1) is consistent provided that (i) the states within the strip do not overlap spatially,

$$\Delta E \nu_0 \xi^D < 1, \quad (\text{B1})$$

and that (ii) the typical variations $\delta\phi$ of the electrostatic energy due to rearrangements of particles within the strip do not exceed the width ΔE of the strip,

$$\delta\phi \sim (\nu_0 \Delta E)^{1/D} \frac{e^2}{\kappa} < \Delta E. \quad (\text{B2})$$

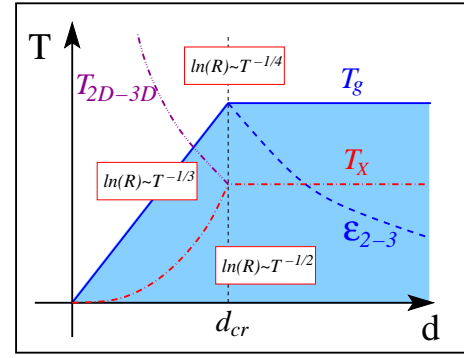


FIG. 10: (Color online) Phase diagram of electron glasses as a function of temperature and film thickness. The dash-dotted lines labeled T_X red (light grey) and T_{2D-3D} purple (dark grey) indicate the crossover between different hopping regimes. The solid lines separate the ergodic high temperature phase from the glass phase where memory effects and aging are observable. The dashed line indicates the temperature and energy scale below which the density of states assumes a linear shape characteristic for two dimensions.

The conditions (B1) and (B2) can be satisfied simultaneously if

$$z = \frac{e^2}{\kappa} \nu_0 \xi^{D-1} < 1, \quad (\text{B3})$$

or, in other words, if the level spacing within a localization volume is larger than the Coulomb interaction strength on the scale of the localization length.

APPENDIX C: THE CROSSOVER FROM 2D TO 3D

In this appendix we discuss the crossover thickness d_{cr} below which a sample should be considered two-dimensional. In particular, we show that the crossover from a bulk sample to a film occurs around a thickness

$$d_{cr} \sim (\nu_0 e^2 / \kappa)^{-1/2}, \quad (\text{C1})$$

both with respect to transport characteristics and the glass transition. [Using typical values for indium-oxide films ($\nu_0 \approx 10^{32} \text{erg}^{-1} \text{cm}^{-3}$ and $\kappa \approx 30^{58}$) one finds $d_{cr} \sim 100 \text{\AA}$ which is of the order of the typical film thickness ($d = 50 - 200 \text{\AA}$) in most glassy experiments.]

In a thin film, Mott’s variable range hopping law (4) crosses over from the 3-D form ($\log(R) \sim T^{-1/4}$) to the 2-D form ($\log(R) \sim T^{-1/3}$) when the hopping length becomes of the order of the film thickness, which yields the crossover temperature

$$T_{2D-3D} \sim T_M^{(3D)} (\xi/d)^4 \sim T_X^{(3D)} / (\nu_0 d^2 e^2 / \kappa)^4. \quad (\text{C2})$$

A subsequent crossover to the Efros-Shklovskii law takes place at $T_X^{(2D)} = T_X^{(3D)} (\nu_0 d^2 e^2 / \kappa)$, where $T_X^{(3D)}$ denotes the Mott to Efros-Shklovskii crossover temperature for a

bulk sample. The intermediate regime with a 2D-Mott's law is observable only if $d < d_{cr}$.

The crossover from a 3D to a 2D glass transition occurs when the typical distance between thermally active sites at $T = T_g^{(3D)}$ becomes equal to the film thickness, i.e., when

$$R_{T_g} \sim e^2/\kappa T_g^{(3D)} \sim e^2/\kappa T_g^{(2D)} \sim d. \quad (C3)$$

One can easily check that these expressions all become of the same order when $\nu_0 d^2 e^2/\kappa = (d/d_{cr})^2 \approx 1$. Notice that for films with $d < d_{cr}$, the glass transition temperature (9) decreases roughly linearly with thickness since $T_g^{(2D)} \sim \nu_0^{(2D)} \sim d\nu_0$. The phase diagram as a function of temperature and film thickness is summarized in Fig. 10.

APPENDIX D: PERCOLATION THEORY OF HOPPING CONDUCTIVITY

In this appendix we review the percolation theory of hopping conductivity. We consider the network of Miller-Abrahams resistors formed by pairs of sites i and j . In the vicinity of a given low temperature metastable state of the electron glass, the effective resistance of this link is approximately given by

$$R_{ij} \approx R_0 \exp(-2r_{ij}/\xi + \epsilon_{ij}/T) \quad (D1)$$

where

$$\epsilon_{ij} = \begin{cases} |E_i - E_j| - e^2/\kappa r_{ij}, & \text{if } E_i \cdot E_j < 0 \\ \max\{|E_i|, |E_j|\}, & \text{if } E_i \cdot E_j > 0 \end{cases} \quad (D2)$$

and E_i is the energy (with respect to the chemical potential) to remove or add a particle at the site i in the particular metastable state at hand. More precisely, the energies E_i refer to the excitation of quasiparticles (or polarons³³) that carry the hopping current.

In order to find the least resistive percolating path in the resistor network we follow the procedure proposed by Efros et al.³⁷: We consider only resistors with $R_{ij} < R_0 \exp(\chi_c)$ to be active and associate to each of them a disk or ball with diameter r_{ij} . We finally determine the threshold value of χ_c for which the set of disks percolates. The value $R_0 \exp(\chi_c)$ is a good estimate of the resistivity to exponential accuracy.

To solve this problem analytically, one needs to know the probability $F(\omega, r)$ per unit energy and volume to find a pair of sites (i, j) with $r_{ij} = r$ and $\epsilon_{ij} = \omega$. Under the assumption that the site energies E_i are independently distributed according to a single-quasiparticle density of states $\rho(E)$, we obtain

$$F(\omega, r) = \frac{1}{2} \int \rho(E_1) \rho(E_2) \delta(\epsilon_{12} - \omega) dE_1 dE_2. \quad (D3)$$

With the help of the pair distribution function the above percolation problem reduces to that of a set of balls with different radii. Assuming that the critical volume fraction of the balls, Θ_D , is an approximate invariant of temperature, only dependent on dimensionality, we finally have

to solve the equation

$$\Theta_D = \int d\omega d^D r V_D \left(\frac{r}{2}\right)^D F(\omega, r) \theta(\chi_c - \frac{\omega}{T} - \frac{2r}{\xi}), \quad (D4)$$

where V_D is the volume of a D -dimensional unit sphere. The above invariance principle yields $\Theta_2 \approx 1.26^{64}$ and $\Theta_3 \approx 0.23^{37}$. Comparison with other percolation criteria, in particular in the Mott regime^{32,65,66}, indicate that in $2D$ a slightly smaller value $\Theta_2 \approx 1$ yields results closer to the numerically found percolation threshold. In the main part of the paper we therefore used the latter value.

In order to efficiently implement the percolation criterion for an arbitrary density of states, as obtained, e.g., after the sudden application of a gate voltage, it is convenient to introduce the functions

$$F_{ph}(E) = 2 \int_0^E d\epsilon \rho(\epsilon) \rho(\epsilon - E) \quad (D5)$$

$$F_{pp}(E) = \rho(E) \int_0^E d\epsilon \rho(\epsilon) \quad (D6)$$

$$F_{hh}(E) = \rho(-E) \int_{-E}^0 d\epsilon \rho(\epsilon) \quad (D7)$$

and $\Phi_{\alpha\beta}(E) = \int_0^E d\epsilon F_{\alpha\beta}(\epsilon)$ with $\alpha, \beta \in \{p, h\}$, in terms of which the percolation criterion (D4) can be rewritten as

$$\Theta_D = \int_0^{\xi\chi_c/2} d^D r V_D \left(\frac{r}{2}\right)^D \cdot [\Phi_{pp}(T(\chi_c - 2r/\xi)) + \Phi_{hh}(T(\chi_c - 2r/\xi)) + \Phi_{ph}(T(\chi_c - 2r/\xi) + e^2/\kappa r) - \Phi_{ph}(e^2/\kappa r)]. \quad (D8)$$

For completeness we report the standard expressions that one obtains in the limiting case of a constant density of states ($\rho(\epsilon) \equiv \nu_0$) and high temperatures ($T \gg T_X$, Mott regime), and in presence of an Efros-Shklovskii pseudogap, $\rho(\epsilon) = \alpha_D (\kappa/e^2)^D \epsilon^{D-1}$, ($T < T_X$). In these cases the above criterion is readily evaluated analytically and yields the threshold values

$$\chi_c = \left(\frac{T_M^D}{T}\right)^{1/(D+1)}, \quad (\text{Mott}) \quad (D9)$$

$$\chi_c = \left(\frac{T_{ES}^D}{T}\right)^{1/2}, \quad (\text{Efros-Shklovskii}) \quad (D10)$$

with

$$T_M^{(D)} = \frac{C_M^{(D)}}{\nu_0 \xi^D} \quad (D11)$$

$$T_{ES}^{(D)} = C_{ES}^{(D)} \frac{e^2}{\kappa \xi}. \quad (D12)$$

The numerical constants $C_M^{(D)}$ depend on the value of Θ_D , while $C_{ES}^{(D)}$ increases with the value of Θ_D/α_D^2 . In the main text we used $\Theta_2 = 1$.

- ¹ J. Davies, P. Lee, and T. Rice, Phys. Rev. Lett. **49**, 758 (1982).
- ² M. Grünewald, B. Pohlmann, L. Schweitzer, and D. Würtz, J. Phys. C **15**, L1153 (1982).
- ³ J. Davies, P. Lee, and T. Rice, Phys. Rev. B **29**, 4260 (1984).
- ⁴ M. Pollak, Philos. Mag. B **50**, 265 (1984).
- ⁵ D. Monroe, A.C. Gossard, J.H. English, B. Golding, and W.H. Haemmerle, Phys. Rev. Lett. **59**, 1148 (1987).
- ⁶ M. Ben-Chorin, Z. Ovadyahu, and M. Pollak, Phys. Rev. B **48**, 15025 (1993).
- ⁷ A. Vaknin, Z. Ovadyahu, and M. Pollak, Phys. Rev. Lett. **81**, 669 (1998).
- ⁸ A. Vaknin, Z. Ovadyahu, and M. Pollak, Phys. Rev. Lett. **84**, 3402 (2000).
- ⁹ V. Orlyanchik and Z. Ovadyahu, Phys. Rev. Lett. **92**, 066801 (2004).
- ¹⁰ Z. Ovadyahu, Philos. Mag. B-Phys. Condens. Matter Stat. Mech. Electron. Opt. Magn. Prop. **81**, 1225 (2001).
- ¹¹ Z. Ovadyahu and M. Pollak, Phys. Rev. B **68**, 184204 (2003).
- ¹² A. Vaknin, Z. Ovadyahu, and M. Pollak, Phys. Rev. B **65**, 134208 (2002).
- ¹³ C.J. Adkins, J.D. Benjamin, J.M.D. Thomas, J.W. Gardner, and A.J. McGeown, J. Phys. C **17**, 4633 (1984).
- ¹⁴ E. Bielejec and W. Wu, Phys. Rev. Lett. **87**, 256601 (2001).
- ¹⁵ T. Grenet, Eur. Phys. J. B **32**, 275 (2003).
- ¹⁶ G. Martinez-Arizala, D.E. Grupp, C. Christiansen, A.M. Mack, N. Markovic, Y. Seguchi, and A.M. Goldman, Phys. Rev. Lett. **78**, 1130 (1997).
- ¹⁷ G. Martinez-Arizala, C. Christiansen, D.E. Grupp, N. Markovic, A.M. Mack, and A.M. Goldman, Phys. Rev. B **57**, R670 (1998).
- ¹⁸ T. Grenet, phys. stat. sol. (c) **1**, 9 (2004).
- ¹⁹ A. Vaknin, Z. Ovadyahu, and M. Pollak, Europhys. Lett. **42**, 307 (1998).
- ²⁰ S. Bogdanovich and D. Popovic, Phys. Rev. Lett. **88**, 236401 (2002).
- ²¹ J. Jaroszynski, D. Popovic, and T. M. Klapwijk, Phys. Rev. Lett. **89**, 276401 (2002).
- ²² M. Pollak, Disc. Faraday Soc. **50**, 13 (1970).
- ²³ A. L. Efros and B. I. Shklovskii, J. Phys. C **8**, L49 (1974).
- ²⁴ A. L. Efros, J. Phys. C **9**, 2021 (1976).
- ²⁵ A. Pastor and V. Dobrosavljević, Phys. Rev. Lett. **83**, 4642 (1999).
- ²⁶ M. Müller and L. B. Ioffe, Phys. Rev. Lett. **93**, 256403 (2004).
- ²⁷ S. Pankov and V. Dobrosavljević, Phys. Rev. Lett. **94**, 046402 (2005).
- ²⁸ A. Zabrodskii, Philos. Mag. B-Phys. Condens. Matter Stat. Mech. Electron. Opt. Magn. Prop. **81**, 1131 (2001).
- ²⁹ *Physical aging in Amorphous Polymers and other materials*, edited by L. C. E. Struick (Elsevier, Houston, 1978).
- ³⁰ P. Nordblad and P. Svedlindh, in *Spin Glasses and Random Fields*, edited by A. P. Young (World Scientific, Singapore, 1998).
- ³¹ A. Efros and B. Shklovskii, in *Electron-Electron interaction in disordered systems*, edited by A. Efros and M. Pollak (North-Holland, Amsterdam, 1985).
- ³² B. Shklovskii and A.L.Efros, *Electronic properties of doped semiconductors* (Springer, Heidelberg, 1984).
- ³³ “Polaron” excitations consist in the change of occupation on one site, and a small number of short hops of neighboring particles that decrease the energy cost for the local charge excitation³¹.
- ³⁴ V. Ambegaokar, B. I. Halperin, and J. S. Langer, Phys. Rev. B **4**, 2612 (1971).
- ³⁵ B. I. Shklovskii and A. L. Efros, Zh. Eksp. Theor. Fiz. **60**, 867 (1971). (Sov. Phys. JETP **33**, 468 (1971)).
- ³⁶ M. Pollak, J. Non-Cryst. Solids **11**, 1 (1972).
- ³⁷ A. L. Efros, V. L. Nguyen, and B. I. Shklovskii, Solid State Commun. **32**, 851 (1979).
- ³⁸ A. Aharony, Y. Zhang, and M. P. Sarachik, Phys. Rev. Lett. **68**, 3900 (1992).
- ³⁹ Y. Meir, Phys. Rev. Lett. **77**, 5265 (1996).
- ⁴⁰ J. Massey and M. Lee, Phys. Rev. Lett. **75**, 4266 (1995).
- ⁴¹ M. Lee, J. Massey, V. Nguyen, and B. Shklovskii, Phys. Rev. B **60**, 1582 (1999).
- ⁴² W. Teizer, F. Hellman, and R. Dynes, Phys. Rev. Lett. **85**, 848 (2000).
- ⁴³ B. Sandow, K. Gloos, R. Rentzsch, A.N. Ionov, and W. Schirmacher, Phys. Rev. Lett. **86**, 1845 (2001).
- ⁴⁴ V. Butko, J. DiTusa, and P. Adams, Phys. Rev. Lett. **84**, 1543 (2000).
- ⁴⁵ V. Y. Butko, J. F. DiTusa, and P. W. Adams, Phys. Rev. Lett. **85**, 162 (2000).
- ⁴⁶ V. Y. Butko and P. Adams, Nature **409**, 161 (2001).
- ⁴⁷ M. Lee, Phys. Rev. Lett. **93**, 256401 (2004).
- ⁴⁸ F. Ladieu, F. Bert, V. Dupuis, E. Vincent, and J. Hammann, J. Phys. C **16**, S735 (2004).
- ⁴⁹ A. Perez-Garrido, M. Ortuno, A. Diaz-Sanchez, and E. Cuevas, Phys. Rev. B **59**, 5328 (1999).
- ⁵⁰ D. Menashe, O. Biham, B. Laikhtman, and A. Efros, Europhys. Lett. **52**, 94 (2000).
- ⁵¹ D. Menashe, O. Biham, B. Laikhtman, and A. Efros, Phys. Rev. B **64**, 115209 (2001).
- ⁵² D. Tsigankov, E. Pazy, B. Laikhtman, and A. Efros, Phys. Rev. B **68**, 184205 (2003).
- ⁵³ D. Gempel, Europhys. Lett. **66**, 854 (2004).
- ⁵⁴ A. B. Kolton, D. R. Gempel, and D. Dominguez, Phys. Rev. B **71**, 024206 (2005).
- ⁵⁵ E. R. Grannan and C. C. Yu, Phys. Rev. Lett. **71**, 3335 (1993).
- ⁵⁶ M. Overlin, L. Wong, and C. Yu, Phys. Rev. B **70**, 214203 (2004).
- ⁵⁷ M. Müller and E. Lebanon, cond-mat/0508703, to be published in J. Phys. France IV (2005).
- ⁵⁸ Z. Ovadyahu, private communication.
- ⁵⁹ E. Helgren, N. Armitage, and G. Gruner, Phys. Rev. B **69**, 014201 (2004).
- ⁶⁰ D. Dalidovich and V. Dobrosavljević, Phys. Rev. B **66**, 081107 (2002).
- ⁶¹ V. Dobrosavljević, D. Tanasković, and A. Pastor, Phys. Rev. Lett. **90**, 016402 (2003).
- ⁶² Z. Ovadyahu, Phys. Rev. B **47**, 6161 (1993).
- ⁶³ O. Cohen and Z. Ovadyahu, Phys. Rev. B **50**, 10442 (1994).
- ⁶⁴ V. L. Nguyen, Sov. Phys. Semicond. **18**, 207 (1984).
- ⁶⁵ C. H. Seager and G. E. Pike, Phys. Rev. B **10**, 1435 (1974).
- ⁶⁶ G. E. Pike and C. H. Seager, Phys. Rev. B **10**, 1421 (1974).